

Multiphase Level-Set Loss for Semi-Supervised and Unsupervised Segmentation with Deep Learning

Boah Kim and Jong Chul Ye, *Senior Member, IEEE*

Abstract—Recent state-of-the-art image segmentation algorithms are mostly based on deep neural network, thanks to its high performance and fast computation time. However, these methods are usually trained in a supervised manner, which requires large number of high quality ground-truth segmentation masks. On the other hand, classical image segmentation approaches such as level-set methods are still useful to help generation of segmentation masks without labels, but these algorithms are usually computationally expensive and often have limitation in semantic segmentation. In this paper, we propose a novel multiphase level-set loss function for deep learning-based semantic image segmentation without or with small labeled data. This loss function is based on the observation that the softmax layer of deep neural networks has striking similarity to the characteristic function in the classical multiphase level-set algorithms. We show that the multiphase level-set loss function enables semi-supervised or even unsupervised semantic segmentation. In addition, our loss function can be also used as a regularized function to enhance supervised semantic segmentation algorithms. Experimental results on multiple datasets demonstrate the effectiveness of the proposed method.

Index Terms—Semi-supervised learning, unsupervised learning, semantic segmentation, multiphase level-set loss

I. INTRODUCTION

SEMANTIC image segmentation is to assign a semantic label to every pixel in the image. Since the image segmentation can be applied to various applications such as object detection [1] and medical image analysis [2]–[4], the segmentation study has been one of the core topics in computer vision.

Recently, deep learning approaches for semantic segmentation have been developed and successfully demonstrated the state-of-the-art performance [5], [6]. A majority of the segmentation works are based on convolutional neural networks (CNN), and they are usually trained in a supervised manner that requires large amount of data with high quality pixel-wise labels [7]–[10]. However, generating segmentation masks is time consuming and can be difficult in certain domains. To overcome this issue, weakly/semi-supervised semantic segmentation methods have been studied in these days. These methods are often under the assumption that training data have various supervisory annotations such as image-level labels [11]–[14] and bounding-box labels [15], or the small number of strongly annotated data.

On the other hand, classical variational image segmentation methods are typically implemented in an unsupervised

B. Kim and J.C. Ye are with the Department of Bio and Brain Engineering, Korea Advanced Institute of Science and Technology (KAIST), Daejeon 34141, Republic of Korea (email: {boahkim, jong.ye}@kaist.ac.kr).

manner, by minimizing a specific energy function so that it can cluster image pixels into several classes [16]–[18]. Since these methods produce pixel-wise prediction without ground-truth, they have extensively used for classical medical image segmentation [19], [20]. Unfortunately, these algorithms are usually computationally expensive and have limitation in semantic image segmentation, so recent segmentation studies have been mainly focused on convolutional neural network (CNN) approaches which are seemingly disconnected from classical approaches.

One of the most important contributions of this paper is, however, to show that the classical wisdom is indeed useful to improve the performance of the CNN-based semantic segmentation, specifically for the unfavorable situation where the training data is not sufficient.

In particular, inspired by the multiphase level-set framework [21], here we propose a novel *multiphase level-set loss* that can be easily employed in CNN-based segmentation algorithms. Because the multiphase level-set methods perform segmentation based on the pixel statistics, the level set loss can exploit the complementary information from the semantic information in the existing CNN-based segmentation algorithms. This property of the proposed loss naturally leads to the CNN-based semi-supervised or unsupervised learning even without ground-truth labels or bounding box annotations. Moreover, for the supervised learning setting, our loss function can be used as a novel regularized function to enhance the performance of the neural network by considering image pixel statistics. Experiments on various datasets verify that the level-set framework and deep learning approach can be synergistically combined to improve the segmentation performance.

II. RELATED WORK

A. Variational Image Segmentation

Classical variational approaches consider image segmentation problem as a clustering problem by minimizing energy functions. Representative examples include k-mean [22], [23], mean shift [24], [25], normalized cuts [26], graph cuts [18], and level-set [21], [27], [28]. Among them, here we briefly review one of the successful variational approaches, called the multiphase level-set framework [21].

Multiphase level-set framework The multiphase level-set method by Chen and Vese [21] was proposed to generalize active contour model [29] for piecewise image segmentation into more than two segments [30]. Consider a set $\Phi = [\phi_1 \cdots \phi_p]$, where $\phi_i : \Omega \rightarrow \mathbb{R}$ denotes a level function from an image

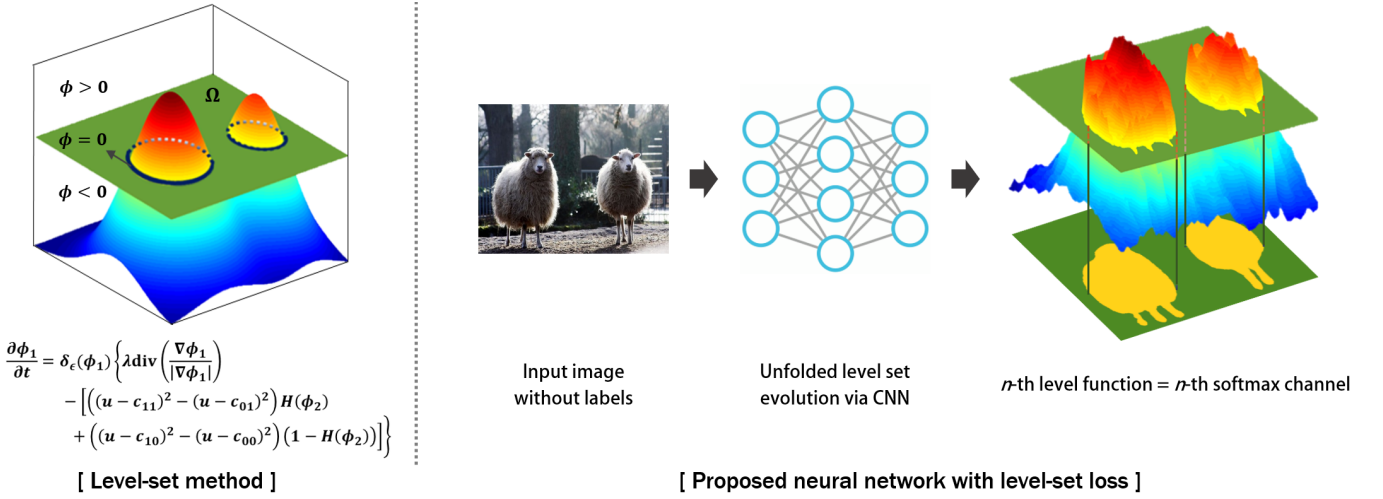


Fig. 1: The overall image segmentation process of the proposed method. A deep neural network can take unlabeled images X_U as well as the pixel-level annotated images X_L . For the input images X_U , the network can be trained by both the existing loss function $L_{segment}$ and the proposed multiphase level-set loss function L_{level} . For the unlabeled input X_U , the network parameters are updated by minimizing L_{level} .

domain Ω to the real number that represents the height of the level-set. We also define the vector Heaviside function [21]:

$$H(\Phi) = [H(\phi_1) \quad \dots \quad H(\phi_p)], \quad (1)$$

where $H(\phi) = 1$ when $\phi > 0$ or $H(\phi) = 0$, otherwise. Using this definition, we can generate 2^p possibilities of the vector Heaviside function values to construct an index set I . Here, N denotes the number of distinct classes within Ω , i.e. $N = |I|$, and our goal is to assign N -class labels for each pixel.

Then, for a given image measurement $u(\mathbf{r})$ for $\mathbf{r} \in \Omega$, the energy function for the multiphase level-set method is given by [21]:

$$\begin{aligned} \mathcal{L}_{level}(\chi; u) = & \sum_{\omega \in I} \int_{\Omega} \|u(\mathbf{r}) - c_{\omega}\|^2 \chi_{\omega}(\mathbf{r}) d\mathbf{r} \\ & + \lambda \sum_{\omega \in I} \int_{\Omega} |\nabla \chi_{\omega}(\mathbf{r})| d\mathbf{r}, \end{aligned} \quad (2)$$

where $\chi_{\omega} := \chi(\Phi)$ denotes the characteristic function for each class element $\omega \in I$ and

$$c_{\omega} = \frac{\int_{\Omega} u(\mathbf{r}) \chi_{\omega}(\mathbf{r}) d\mathbf{r}}{\int_{\Omega} \chi_{\omega}(\mathbf{r}) d\mathbf{r}}. \quad (3)$$

In order to simplify the model, the authors in [21] replaced the last length-related term in (2) by

$$\sum_{i=1}^p \int_{\Omega} |\nabla H(\phi_i)|. \quad (4)$$

This leads to the Euler-Lagrangian equation for the level function. For example, for the classification of $N = 4$ levels with two level functions (i.e. $p = 2$ and $I = \{00, 01, 10, 11\}$),

the Euler-Lagrangian equations for the level functions are given by:

$$\begin{aligned} \frac{\partial \phi_1}{\partial t} = & \delta_{\epsilon}(\phi_1) \left\{ \lambda \operatorname{div} \left(\frac{\nabla \phi_1}{|\nabla \phi_1|} \right) \right. \\ & \left. - \left[((u - c_{11})^2 - (u - c_{01})^2) H(\phi_2) \right. \right. \\ & \left. \left. + ((u - c_{10})^2 - (u - c_{00})^2)(1 - H(\phi_2)) \right] \right\}, \end{aligned} \quad (5)$$

$$\begin{aligned} \frac{\partial \phi_2}{\partial t} = & \delta_{\epsilon}(\phi_2) \left\{ \lambda \operatorname{div} \left(\frac{\nabla \phi_2}{|\nabla \phi_2|} \right) \right. \\ & \left. - \left[((u - c_{11})^2 - (u - c_{10})^2) H(\phi_1) \right. \right. \\ & \left. \left. + ((u - c_{01})^2 - (u - c_{00})^2)(1 - H(\phi_1)) \right] \right\}, \end{aligned} \quad (6)$$

where δ_{ϵ} denotes an approximation to the one-dimensional Dirac delta function. For multichannel images such as color images, this energy function (2) can be easily extended by defining $u(\mathbf{r})$ and c_{ω} as vectors composed of each channel values at $\mathbf{r} \in \Omega$. The Euler-Lagrangian equation can be then obtained by directly minimizing (2) with respect to Φ :

Thanks to the high-dimensional lifting nature of the level functions, the multiphase level-set approach can successfully segment spatially separated regions of the same class.

B. CNN-Based Image Segmentation

1) *Supervised Learning Approach:* When the pixel-wise annotations are available, deep neural network-based semantic segmentation approaches have become the main workhorses for modern segmentation techniques thanks to their high performance and fast runtime complexity [5], [6]. Since fully convolutional networks (FCNs) [9] generate output map with same size of the input, various deep learning methods using FCNs are studied for semantic image segmentation [7], [10], [31]–[33].

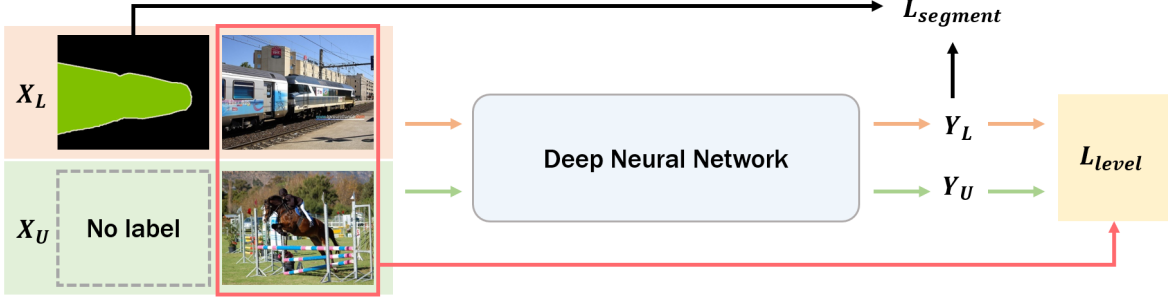


Fig. 2: The overall image segmentation process of the proposed method. A deep neural network can take unlabeled images X_U as well as the pixel-level annotated images X_L . For the input images X_U , the network can be trained by both the existing loss function $L_{segment}$ and the proposed multiphase level-set loss function L_{level} . For the unlabeled input X_U , the network parameters are updated by minimizing L_{level} .

2) *Weakly/semi-supervised Learning Approach*: Although the supervised learning methods outperform the semantic segmentation, labeling images with pixel-level annotations is difficult to obtain for enormous amount of data. To address this issue, Qi et al. [14] develop a unified method of semantic segmentation and object localization with only image-level signals. Papandreou et al. [12] present expectation-maximization (EM) method to predict segmentation maps by adding image-level annotated images. Hong et al. [11] propose a decoupled architecture to learn classification and segmentation networks separately using the data with image-level supervision and pixel-level annotations. Also, Hung et al. [34] develop an adversarial learning method for segmentation, which use the output of a discriminator as the weak labels to leverage unlabeled images.

3) *Unsupervised Learning Approach*: In addition, unsupervised learning methods for semantic segmentation have been studied to segment the data without any ground-truth segmentation masks [35], [36]. Several recent works present unsupervised approaches using classical optimization-based algorithms as a constraint functions [37]–[39].

C. Our Contribution

- In contrast to the classical multiphase level-set approach [21], which relies on computational expensive level function evolution by the Euler-Lagrangian equation, in the proposed method the level function evolution is learned using a neural network because our multiphase level-set loss allows the back-propagation.
- Unlike the existing weakly/semi-supervised segmentation [11], [12], [14], [34], the proposed algorithm does not require the weak-labeled supervision for unlabeled data, but still uses these unlabeled images as elements of the training data thanks to the level-set loss that depends on pixel statistics. Thus, the proposed method greatly alleviates the task of manual annotation.
- While the existing CNN-based unsupervised learning methods [35]–[39] usually require complex pre- and /or post-processing, this post-processing step is not necessary and the algorithm only requires an addition of a multiphase level-set loss.

- While the combination of level-set method with CNN segmentation can be found in Kristiadi [40] and Le [41], these authors trained the networks in a supervised manner and used the level-set method for refinement step of segmentation map. In contrast, our algorithm is derived by directly unrolling level-set evolution using a CNN so that it can be used for network training under semi-, unsupervised- and fully supervised setting.
- When the multiphase level-set loss can be used as a data-adaptive regularized function in a fully supervised segmentation algorithm, the multiphase level-set loss allows the network to better adapt to the specific image statistics to further improve segmentation performance.

III. THEORY

A. Unfolded Level-Set Evolution, Level-Set Loss

A discrete implementation of the level function evolution (5) and (6) can be represented by

$$\phi_1^{k+1} = F(\phi_1^k, \phi_2^k, u; \lambda^k, \epsilon^k), \quad \phi_2^{k+1} = G(\phi_1^k, \phi_2^k, u; \lambda^k, \epsilon^k) \quad (7)$$

where ϕ_i^k and (λ^k, ϵ^k) refer to the i -th level functions and the hyper-parameters, respectively, at the k -th time evolution. Here, the curvature flow term $\text{div} \left(\frac{\nabla \phi_1}{|\nabla \phi_1|} \right)$ in (5) and (6) are nonlinear with respect to ϕ_1 . Inspired by the Learned iterative soft-thresholding algorithm (LISTA) [42], we therefore use a time unfolded version of the level set evolution block (7), truncated to a fixed number of iterations. Specifically, the λ^k, ϵ^k for each block are learned as network weights so as to minimize the approximation error to the optimal sparse code on a given dataset. Furthermore, the nonlinearity from curvature flow is interpreted as the nonlinearity in deep neural networks.

Moreover, instead of using the simplification in (4), we are interested in the derivation of the unfolded level-set evolution by minimizing the original energy function (2). In this regard, one of the important observations is that the softmax layer of deep neural network can be used as a differentiable approximation of the characteristic function. Specifically, the n -th

channel softmax output from a neural network is defined as follows:

$$y_n^\Theta(\mathbf{r}) = \frac{e^{z_n^\Theta(\mathbf{r})}}{\sum_{i=1}^N e^{z_i^\Theta(\mathbf{r})}}, \quad n = 1, 2, \dots, N, \quad (8)$$

where $\mathbf{r} \in \Omega$, and $z_i^\Theta(\mathbf{r})$ denotes the network output at \mathbf{r} from the preceding layer before the softmax, and Θ refers to the parameter of neural network. The output value of (8) is close to 1 when the pixel value at \mathbf{r} belongs to the class n . Furthermore, it is easy to show that

$$\sum_{n=1}^N y_n^\Theta(\mathbf{r}) = 1, \quad \forall \mathbf{r} \in \Omega, \quad (9)$$

which is basically identical to the characteristic function property in the multiphase level-set framework:

$$\sum_{\omega \in I} \chi_\omega(\mathbf{r}) = 1, \quad \forall \mathbf{r} \in \Omega. \quad (10)$$

This similarity clearly implies that the softmax function output can work as a differentiable version of the characteristic function for the class membership. Therefore, without using the replacement (4), we propose to use the following multiphase level-set energy function as an objective function:

$$\begin{aligned} \mathcal{L}_{level}(\Theta; x) = & \sum_{n=1}^N \int_{\Omega} |x(\mathbf{r}) - c_n^\Theta|^2 y_n^\Theta(\mathbf{r}) d\mathbf{r} \\ & + \lambda \sum_{n=1}^N \int_{\Omega} |\nabla y_n^\Theta(\mathbf{r})| d\mathbf{r} \end{aligned} \quad (11)$$

with

$$c_n^\Theta = \frac{\int_{\Omega} x(\mathbf{r}) y_n^\Theta(\mathbf{r}) d\mathbf{r}}{\int_{\Omega} y_n^\Theta(\mathbf{r}) d\mathbf{r}}, \quad (12)$$

where $x(\mathbf{r})$ is the input, $y_n^\Theta(\mathbf{r})$ is the output of softmax layer in (8), and Θ refers to the learnable network parameters. Note that (11) is differentiable with respect to Θ . Therefore, the unfolded level set evolution for y_n^Θ can be implemented using a neural network with the weight Θ as shown in Fig. 1.

B. Application of Multiphase Level-Set

While Fig. 1 shows the applications of the proposed method for unsupervised segmentation problems, the application of the level set loss is quite general and can be combined with any supervised, semi-supervised and unsupervised segmentation algorithm. Specifically, Fig. 2 illustrates a typical use of the proposed level-set loss. Here, a deep neural network can be any existing segmentation network, which takes input images with or without pixel-level annotated data and generates segmentation maps. Only difference is the addition of the level set loss \mathcal{L}_{level} . Here, we describe the various application of the multiphase level-set loss in more detail.

1) *Semi-Supervised Segmentation*: For the semi-supervised learning, we apply the conventional segmentation loss function for pixel-level annotated data and the multiphase level-set loss for unlabeled data so that the deep neural network can be trained without any estimated or weak supervisory labels.

Specifically, let N for the number of segmentation classes. In order to use both labeled and unlabeled data, the loss function for network training is designed as following:

$$loss = \alpha \mathcal{L}_{segment} + \beta \mathcal{L}_{level}, \quad (13)$$

where

$$\alpha = \begin{cases} 1, & \text{if the input has labels} \\ 0, & \text{otherwise,} \end{cases}$$

and β is a hyper-parameter. Here, $\mathcal{L}_{segment}$ is usually the cross-entropy function defined by:

$$\mathcal{L}_{CE} = -\frac{1}{P} \sum_{i=1}^P \sum_{n=1}^N g_i^n \log y_i^n, \quad (14)$$

where y_i^n denotes the predicted probability of voxel i belongs to class n (background, object) in the segmentation map, g_i^n denotes the segmentation ground-truth label, and P is the number of pixels of input. Accordingly, when the network takes the input that does not have pixel-wise label, the network is trained only by the multiphase level-set loss that segments objects with automatically designed level-sets. On the other hand, when the network takes the labeled data, the network is trained to segment specific regions and classify those categories using both the level-set loss and the conventional segmentation loss.

2) *Unsupervised Segmentation*: Since our multiphase level-set loss in deep learning estimate the cluster based on the pixel statistics, the unsupervised-learning-based semantic segmentation is also possible. In particular, the loss function for the unsupervised learning algorithm is defined using the formula (13) with $\alpha = 0$. By minimizing this loss, the neural network achieves level-set evolution and centroid update for segmented regions through training phase. At the inference stage, the network automatically segment objects in images with their class information.

3) *Supervised Segmentation*: In this case, we use $\alpha = 1$ in (13). Unlike conventional supervised learning method that computes $\mathcal{L}_{segment}$ only with the network output and segmentation label, the neural network is trained to consider input image statistics as well as semantic information. By computing the relationship between the input distribution and segmentation regions with the multiphase level-set loss, the proposed method performs segmentation in more detail.

IV. METHOD

A. Datasets

1) *PASCAL VOC 2012*: To evaluate the semantic segmentation performance of our model on the daily captured natural images, we use PASCAL VOC 2012 segmentation benchmark [43], consisting of 20 object classes. We also use the extra annotated images from Segmentation Boundaries Dataset (SBD) [44] for training, so that we obtain an augmented training

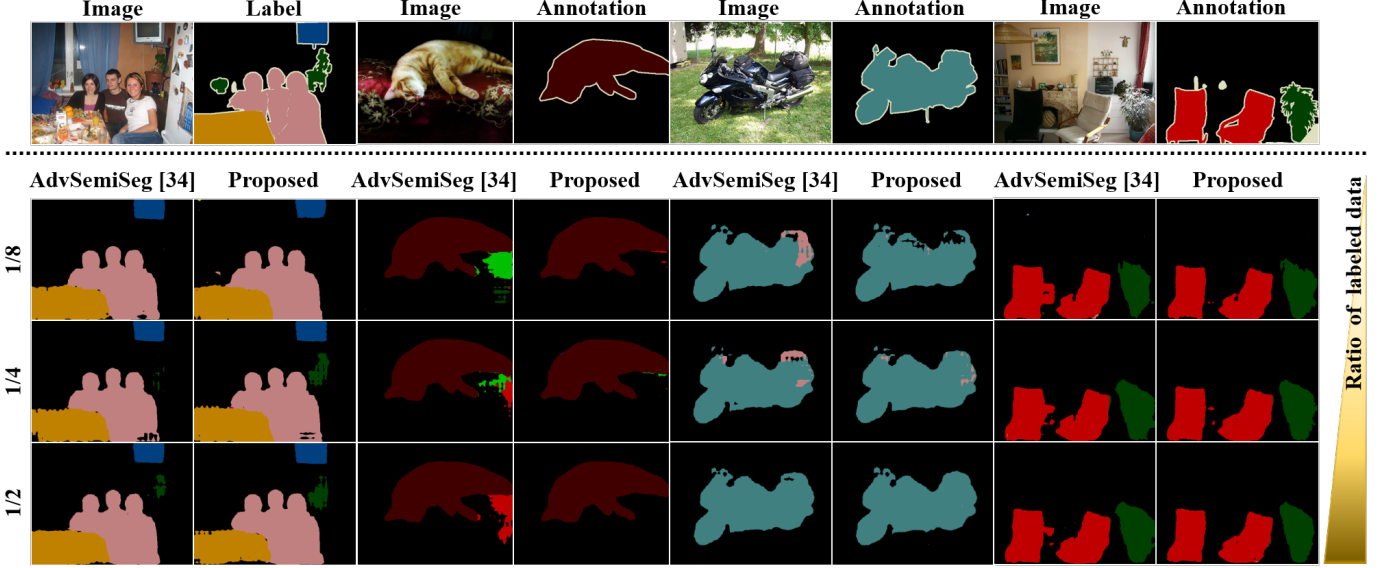


Fig. 3: Qualitative results from our proposed method and AdvSemiSeg [34] using the PASCAL VOC 2012 *val* set. We randomly sample 1/8, 1/4, 1/2 images as labeled data, and train the models with both labeled data and the rest of training images as unlabeled data. We train the model of [34] with our multiphase level-set loss \mathcal{L}_{level} , and compare the proposed method to the [34].

dataset of 10,582 images. We randomly scale and crop the images into 321×321 during training, and evaluate our semi-supervised algorithm on the validation set with 1449 images.

2) *LiTS 2017*: To apply our method to medical image segmentation, we used Liver Tumor Segmentation Challenge (LiTS) dataset [45]. This provides 201 contrast-enhanced 3D abdominal CT scans and segmentation labels for liver and tumor regions. All volumes contains a number of axial slices with a resolution of 512×512 pixels. We divide the data into 118 scans for the network training and 13 scans for the validation. We clip the intensity values to the range [-124, 276] HU to ignore irrelevant details and normalize the images to $[0, 1]$ by the maximum value of data. Also, we downsample the images into 256×256 .

3) *BRATS 2015*: The multimodal brain tumor image segmentation benchmark (BRATS) [46] contains 274 MR scans from different patients-histological diagnosis. Each scans has skull-stripped four MRI sequences: T1-weighted (T1), T1 with gadolinium enhancing contrast (T1c), T2-weighted (T2) and FLAIR. All training data with the size $240 \times 240 \times 155$ have the manual segmentation labels for several types of brain tumor. We train the model for the complete tumor segmentation using 249 training data and evaluate our method on the 25 test set.

4) *BSDS500*: The Berkeley Segmentation Database (BSDS500) provides 200, 100, 200 images for the training, validation, and test images with human-annotated labels, respectively. We resize all training images to $512 \times 512 \times 3$.

B. Network Implementation

1) *Object Segmentation in Natural Images*: On the PASCAL VOC 2012 dataset, we train our model in a semi-supervised setting. For the semi-supervised learning, we employ the AdvSemiSeg [34] that employs adversarial loss and a

modified version of the DeepLab-v2 [5] as a baseline network. This modified DeepLab-v2 does not use the multi-scale fusion, rather the Atrous Spatial Pyramid Pooling (ASPP) method is used in the last layer. We use same parameters of [34] and compute the multiphase level-set loss for the softmax-operated final output.

To demonstrate how our method can convert the existing supervised segmentation network to unsupervised network by simply replacing the semantic loss with the multiphase level-set loss, we add the multiphase level-set loss to the U-Net [10] and train the model without ground truth labels on the BSDS500 dataset. Additionally, in order to show that our loss can improve the existing unsupervised segmentation network, we add the multiphase level-set loss to the model of Backprop [39] and trained the network without labels.

2) *Tumor Segmentation in Medical Images*: For the tumor segmentation on LiTS 2017 and BRATS 2015, we use the improved version of U-Net [47]. This modification comes from the pooling and unpooling layers of the U-Net [10] using the polyphase decomposition: the four neighbor pixels of the input are decomposed into the four channels data with reduced size at the pooling layer, whereas the four reduced size channels are grouped together to an enlarged single channel at the pooling layer. This modification improves the segmentation performance by retaining more details.

C. Training Details

To train the networks in a semi-supervised manner, we randomly divide each training datasets into labeled and unlabeled data with various ratio. We implement the proposed method using the pyTorch library in Python.

For the object segmentation using PASCAL VOC dataset, we trained the proposed model using the Stochastic Gradient

Methods	Ratio of labeled data amount			
	1/8	1/4	1/2	Full
Dilation10 [48]	N/A	N/A	N/A	73.9
AdvSemiSeg [34]	68.87	70.74	72.88	N/A
Proposed	69.30	71.05	72.04	73.58

TABLE I: Quantitative results of object segmentation on the PASCAL VOC 2012 *val* set. We compute the mean intersection-over-union (mean IoU) for all segmentation classes.

Descent (SGD) optimization method. As described in [34], the initial learning rate is set as 2.5×10^{-4} and is decreased with polynomial decay with power of 0.9. We train the model using 20,000 iterations with batch size 10 on two NVIDIA GeForce GTX 1080 Ti.

We also implement our unsupervised learning algorithm on the BSDSS500 dataset. In the training of the U-Net, we use the Adam optimization algorithm with initial learning rate 10^{-5} and batch size 4. We stop the training after 200 epochs. For training of modified Backprop [39], we use SGD algorithm and initialize the parameters with Xavier initialization. We train the network for 500 times and obtain the final segmentation maps.

For the tumor segmentation in medical images, we stack three adjacent slices in a volume as an input, and train the network to generate segmentation masks corresponding to the center slice of the input. We use the Adam optimization method. The initial learning rate is set as 10^{-5} and multiplied by 0.5 after every 20 epochs. Using a single GPU mentioned above, we train the model with batch size 4 for 50 and 40 epochs on each LiTS and BRATS datasets.

V. EXPERIMENTAL RESULTS

A. Semi-Supervised Object Segmentation in Natural Images

1) *Experimental Scenario*: For the network training in a semi-supervised setting, we randomly chose 1/2, 1/4, 1/8 of whole images as labeled data, and use both those sampled images and the rest of training dataset provided by the PASCAL VOC 2012 segmentation benchmark. We add our multiphase level-set loss to the loss function of the AdvSemiSeg [34]. In this experiment, $\mathcal{L}_{segment}$ in (13) is defined as its original loss function in the AdvSemiSeg.

2) *Quantitative evaluation*: Table I shows the evaluation results on the PASCAL VOC 2012 *val* dataset. We use the mean intersection-over-union (mean IoU) as the evaluation metric. We compare the proposed algorithm with AdvSemiSeg [34] in order to verify that the multiphase level-set loss brings comparable segmentation results to the state-of-the-art algorithms. We can see that the proposed method using the multiphase level-set loss improves performance with small labeled data compared to the total training data.

3) *Qualitative evaluation*: Fig. 3 illustrates the segmentation results from our proposed method over different amounts of training data. It shows that the objects segmentation is performed more accurately with increasing the rate of labeled data during training phase compared to AdvSemiSeg [34]. Also, even in the cases of the small number of labeled data,

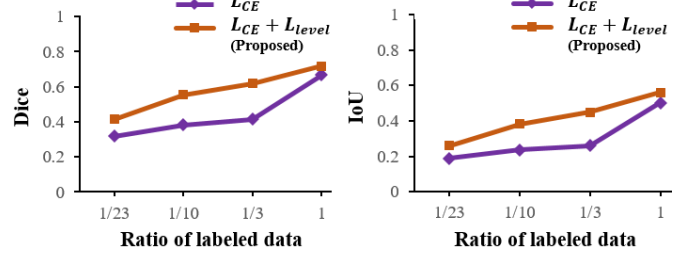


Fig. 4: Quantitative results of liver lesion segmentation by the proposed method using the validation set from LiTS 2017. The comparison was performed using various ratio of labeled data. Left: Dice score. Right: Intersection of Union (IoU) score.

Methods	Dice	Precision	Recall	IoU
U-Net [10]	0.87	0.93	0.81	0.76
Proposed	0.89	0.89	0.87	0.78

TABLE II: Quantitative comparison results of brain tumor segmentation on 25 validation scans of the BRATS dataset. We test our model with 1/4 training labeled data.

we confirm that the objects are segmented in the direction of correct answer thanks to the multiphase level-set loss.

B. Semi-Supervised Tumor Segmentation in Medical Images

1) *Experimental Scenario*: In order to segment liver lesion in CT images effectively on the LiTS dataset, we train two modified U-Nets; the first is to segment a liver from CT abdominal scans, and the second is for lesion segmentation from the segmented liver. We validate the semi-supervised learning algorithm using randomly chosen 1/23, 1/10, 1/3 scans of the full data as labeled data, and the rest of data are used as unlabeled data.

For the tumor segmentation using BRATS dataset, we use the modified U-Net using all three adjacent slices for each MR sequences (T1, T1c, T2, and FLAIR images) as an input. Among the training dataset, we randomly sample 1/4 MR scans of the full data as labeled data for the semi-supervised learning scheme.

To verify the role of multiphase level-set loss as a segmentation function, we compare our method to the supervised learning method by setting $\mathcal{L}_{segment} = \mathcal{L}_{CE}$. With the help of the conventional cross-entropy loss, the proposed semi-supervised learning method can segment specific regions in images without estimated or weakly-annotated labels for the unlabeled data.

2) *Quantitative evaluation*: We evaluate the performance of tumor segmentation using the Dice coefficient, precision, recall, and intersection-over-union (IoU). Fig. 4 shows the scores on the 13 LiTS *val* set according to the ratio of labeled and unlabeled data. The semi-supervised learning method using our proposed multiphase level-set loss on the LiTS data brings significant performance improvement from 10% to 20%, over different amounts of labeled data. As described in Table II, the overall scores from our semi-supervised method on brain tumor segmentation are also higher than the general supervised learning method. We confirm that the multiphase level-set

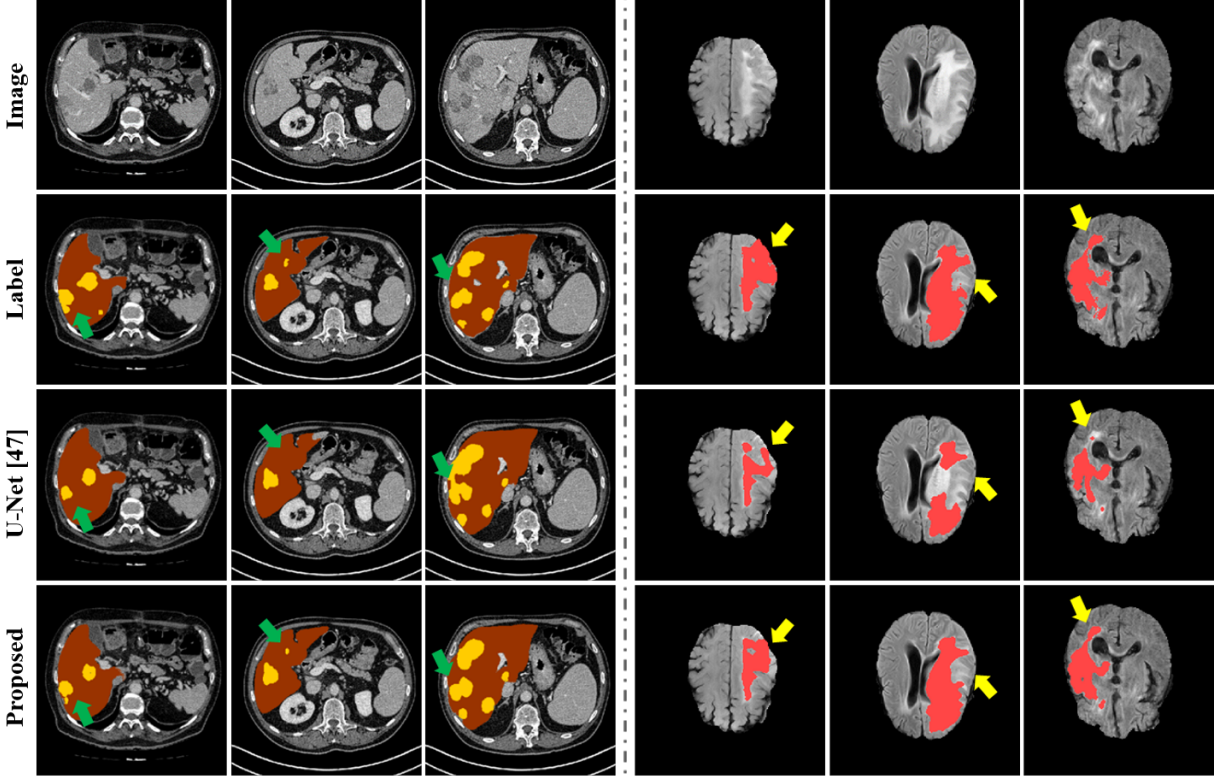


Fig. 5: Qualitative results of the tumor segmentation by the proposed method. Left: results from our method using 1/10 labeled data on the LiTS dataset. Right: results from our method using 1/4 labeled data on the BRATS dataset. First row: center slices of input. Second row: liver lesion segmentation labels. Third row: results from the supervised learning method [10] by \mathcal{L}_{CE} . Fourth row: results from our semi-supervised learning algorithm using \mathcal{L}_{CE} and \mathcal{L}_{level} .

plays a role of regularizer and improves the segmentation performance, when training the network using all training dataset with labels (ratio of labeled data = 1).

3) *Qualitative evaluation*: Fig. 5 illustrates both the predicted liver lesion segmentation maps for CT slices and tumor segmentation maps for MR scans. These results verify that the multiphase level-set loss enables the network to detect boundary of tumor region in more detail. Also, since the level-set loss is computed with pixel-level information, we can observe that tiny and thin tumors are clearly segmented in our method, which are hard to be distinguished with surrounding area.

C. Unsupervised Semantic Segmentation in Natural Images

We train and test our unsupervised learning method on the BSDS500 dataset. The results of our unsupervised method directly verify that the combination of level-set framework and deep neural network improves the performance of semantic segmentation.

1) *Quantitative evaluation*: Table III shows the results of comparisons and our method. We compute the Region Covering (RC), Probabilistic Rand Index (PRI), and Variation of Information (VI) as evaluation metrics. We compare the proposed method against both the classical methods [21], [24], [26] and deep unsupervised learning approaches [39]. We achieve 7% and 4% gain in RC with respect to Level-set [21] and Backprop [39], respectively. Also, we observe

Method	RC	PRI	VI
Level-set [21] (#regions=7)	0.40	0.70	2.72
N-Cuts [26]	0.45	0.78	2.23
Backprop [39]	0.43	0.72	3.19
Backprop [39] + \mathcal{L}_{level}	0.46	0.70	2.27
Proposed	0.47	0.74	2.33

TABLE III: Quantitative results in various metrics according to optimal dataset scale (ODS) on the BSDS500.

that our multiphase level-set loss improves the segmentation performance of the existing unsupervised learning method.

2) *Qualitative evaluation*: Fig. 6 shows visual comparisons of the semantic segmentation results. We confirm that our method segments various foreground objects such as human and animals with higher performance than the comparative methods.

VI. CONCLUSIONS

We propose a novel multiphase level-set loss for deep neural network to learn semantic segmentation in semi-supervised and unsupervised manner. The loss function can be applied for both unlabeled and labeled data, so that the deep neural network learns the segmentation of specific regions with or without small labeled data. Experiments on the various datasets demonstrate high performance of our proposed method.



Fig. 6: Results of unsupervised semantic segmentation using BSDS500 datasets. The first rows are various natural images, and the second and third rows are results from the baseline methods. The third row images are from the Backprop [39] combined with the multiphase level-set loss. The fourth row shows the results from U-Net with the multiphase level-set loss. The results shows that the our multiphase level-set loss improves the performance of the existing methods and also converts the supervised learning algorithms to an unsupervised learning method with the state-of-the art performance.

REFERENCES

- [1] B. Leibe, A. Leonardis, and B. Schiele, “Robust object detection with interleaved categorization and segmentation,” *International journal of computer vision*, vol. 77, no. 1-3, pp. 259–289, 2008.
- [2] J. Lee and A. P. Reeves, “Segmentation of individual ribs from low-dose chest ct,” in *Medical Imaging 2010: Computer-Aided Diagnosis*, vol. 7624. International Society for Optics and Photonics, 2010, p. 76243J.
- [3] Q. A. Salih, A. R. Ramli, R. Mahmud, and R. Wirza, “Brain white and gray matter anatomy of mri segmentation based on tissue evaluation,” *Medscape General Medicine*, vol. 7, no. 2, p. 1, 2005.
- [4] C. Cernazanu-Glavan and S. Holban, “Segmentation of bone structure in x-ray images using convolutional neural network,” *Adv. Electr. Comput. Eng.*, vol. 13, no. 1, pp. 87–94, 2013.
- [5] L.-C. Chen, G. Papandreou, I. Kokkinos, K. Murphy, and A. L. Yuille, “Deeplab: Semantic image segmentation with deep convolutional nets, atrous convolution, and fully connected crfs,” *IEEE transactions on pattern analysis and machine intelligence*, vol. 40, no. 4, pp. 834–848, 2018.
- [6] M. Kampffmeyer, A.-B. Salberg, and R. Jenssen, “Semantic segmentation of small objects and modeling of uncertainty in urban remote sensing images using deep convolutional neural networks,” in *Proceedings of the IEEE conference on computer vision and pattern recognition workshops*, 2016, pp. 1–9.
- [7] V. Badrinarayanan, A. Kendall, and R. Cipolla, “Segnet: A deep convolutional encoder-decoder architecture for image segmentation,” *arXiv preprint arXiv:1511.00561*, 2015.
- [8] H. Noh, S. Hong, and B. Han, “Learning deconvolution network for semantic segmentation,” in *Proceedings of the IEEE international conference on computer vision*, 2015, pp. 1520–1528.
- [9] J. Long, E. Shelhamer, and T. Darrell, “Fully convolutional networks for semantic segmentation,” in *Proceedings of the IEEE conference on computer vision and pattern recognition*, 2015, pp. 3431–3440.
- [10] O. Ronneberger, P. Fischer, and T. Brox, “U-net: Convolutional networks for biomedical image segmentation,” in *International Conference on Medical image computing and computer-assisted intervention*. Springer, 2015, pp. 234–241.
- [11] S. Hong, H. Noh, and B. Han, “Decoupled deep neural network for semi-supervised semantic segmentation,” in *Advances in neural information processing systems*, 2015, pp. 1495–1503.
- [12] G. Papandreou, L.-C. Chen, K. P. Murphy, and A. L. Yuille, “Weakly- and semi-supervised learning of a deep convolutional network for semantic image segmentation,” in *Proceedings of the IEEE international conference on computer vision*, 2015, pp. 1742–1750.
- [13] P. O. Pinheiro and R. Collobert, “Weakly supervised semantic segmentation with convolutional networks,” in *CVPR*, vol. 2, no. 5. Citeseer, 2015, p. 6.
- [14] X. Qi, Z. Liu, J. Shi, H. Zhao, and J. Jia, “Augmented feedback in semantic segmentation under image level supervision,” in *European Conference on Computer Vision*. Springer, 2016, pp. 90–105.
- [15] J. Dai, K. He, and J. Sun, “Boxsup: Exploiting bounding boxes to supervise convolutional networks for semantic segmentation,” in *Proceedings of the IEEE International Conference on Computer Vision*, 2015, pp. 1635–1643.
- [16] P. J. Kumar Baldevbhai and R. Anand, “Color image segmentation using clustering,” *International Journal of Advanced Research in Computer Engineering and Technology*, vol. 1, no. 4, pp. 563–574, 2012.
- [17] J. Shi and J. Malik, “Normalized cuts and image segmentation,” *IEEE Transactions on pattern analysis and machine intelligence*, vol. 22, no. 8, pp. 888–905, 2000.
- [18] Y. Y. Boykov and M.-P. Jolly, “Interactive graph cuts for optimal boundary & region segmentation of objects in nd images,” in *Computer Vision, 2001. ICCV 2001. Proceedings. Eighth IEEE International Conference on*, vol. 1. IEEE, 2001, pp. 105–112.
- [19] S. Liu and J. Li, “Automatic medical image segmentation using gradient and intensity combined level set method,” in *Engineering in Medicine and Biology Society, 2006. EMBS’06. 28th Annual International Conference of the IEEE*. IEEE, 2006, pp. 3118–3121.
- [20] C. Duan, Z. Liang, S. Bao, H. Zhu, S. Wang, G. Zhang, J. J. Chen, and H. Lu, “A coupled level set framework for bladder wall segmentation with application to mr cystography,” *IEEE transactions on medical imaging*, vol. 29, no. 3, pp. 903–915, 2010.
- [21] L. A. Vese and T. F. Chan, “A multiphase level set framework for image segmentation using the mumford and shah model,” *International journal of computer vision*, vol. 50, no. 3, pp. 271–293, 2002.
- [22] N. Dhanachandra, K. Manglem, and Y. J. Chanu, “Image segmentation using k-means clustering algorithm and subtractive clustering algorithm,” *Procedia Computer Science*, vol. 54, pp. 764–771, 2015.
- [23] C. W. Chen, J. Luo, and K. J. Parker, “Image segmentation via adaptive k-mean clustering and knowledge-based morphological operations with

biomedical applications,” *IEEE transactions on image processing*, vol. 7, no. 12, pp. 1673–1683, 1998.

[24] D. Comaniciu and P. Meer, “Mean shift: A robust approach toward feature space analysis,” *IEEE Transactions on pattern analysis and machine intelligence*, vol. 24, no. 5, pp. 603–619, 2002.

[25] G. Beck, T. Duong, H. Azzag, and M. Lebbah, “Distributed mean shift clustering with approximate nearest neighbours.” in *IJCNN*, 2016, pp. 3110–3115.

[26] T. Cour, F. Benezit, and J. Shi, “Spectral segmentation with multiscale graph decomposition,” in *2005 IEEE Computer Society Conference on Computer Vision and Pattern Recognition (CVPR’05)*, vol. 2. IEEE, 2005, pp. 1124–1131.

[27] V. Caselles, F. Catté, T. Coll, and F. Dibos, “A geometric model for active contours in image processing,” *Numerische mathematik*, vol. 66, no. 1, pp. 1–31, 1993.

[28] C. Li, C. Xu, C. Gui, and M. D. Fox, “Distance regularized level set evolution and its application to image segmentation,” *IEEE transactions on image processing*, vol. 19, no. 12, p. 3243, 2010.

[29] T. Chan and L. Vese, “An active contour model without edges,” in *International Conference on Scale-Space Theories in Computer Vision*. Springer, 1999, pp. 141–151.

[30] D. Mumford and J. Shah, “Optimal approximations by piecewise smooth functions and associated variational problems,” *Communications on pure and applied mathematics*, vol. 42, no. 5, pp. 577–685, 1989.

[31] P. Krähenbühl and V. Koltun, “Efficient inference in fully connected crfs with gaussian edge potentials,” in *Advances in neural information processing systems*, 2011, pp. 109–117.

[32] P. F. Christ, M. E. A. Elshaer, F. Ettlinger, S. Tatavarty, M. Bickel, P. Bilic, M. Rempler, M. Armbruster, F. Hofmann, M. DAnastasi *et al.*, “Automatic liver and lesion segmentation in ct using cascaded fully convolutional neural networks and 3d conditional random fields,” in *International Conference on Medical Image Computing and Computer-Assisted Intervention*. Springer, 2016, pp. 415–423.

[33] P. V. Tran, “A fully convolutional neural network for cardiac segmentation in short-axis mri,” *arXiv preprint arXiv:1604.00494*, 2016.

[34] W.-C. Hung, Y.-H. Tsai, Y.-T. Liou, Y.-Y. Lin, and M.-H. Yang, “Adversarial learning for semi-supervised semantic segmentation,” *arXiv preprint arXiv:1802.07934*, 2018.

[35] T. T. Pham, T.-T. Do, N. Sünderhauf, and I. Reid, “Scenecut: Joint geometric and object segmentation for indoor scenes,” in *2018 IEEE International Conference on Robotics and Automation (ICRA)*. IEEE, 2018, pp. 1–9.

[36] C. Wang, B. Yang, and Y. Liao, “Unsupervised image segmentation using convolutional autoencoder with total variation regularization as preprocessing,” in *Acoustics, Speech and Signal Processing (ICASSP), 2017 IEEE International Conference on*. IEEE, 2017, pp. 1877–1881.

[37] X. Xia and B. Kulis, “W-net: A deep model for fully unsupervised image segmentation,” *arXiv preprint arXiv:1711.08506*, 2017.

[38] T. Moriya, H. R. Roth, S. Nakamura, H. Oda, K. Nagara, M. Oda, and K. Mori, “Unsupervised segmentation of 3d medical images based on clustering and deep representation learning,” in *Medical Imaging 2018: Biomedical Applications in Molecular, Structural, and Functional Imaging*, vol. 10578. International Society for Optics and Photonics, 2018, p. 105780.

[39] A. Kanezaki, “Unsupervised image segmentation by backpropagation,” in *2018 IEEE International Conference on Acoustics, Speech and Signal Processing (ICASSP)*. IEEE, 2018, pp. 1543–1547.

[40] A. Kristiadi and P. Pranowo, “Deep convolutional level set method for image segmentation,” *Journal of ICT Research and Applications*, vol. 11, no. 3, pp. 284–298, 2017.

[41] T. H. N. Le, K. G. Quach, K. Luu, C. N. Duong, and M. Savvides, “Reformulating level sets as deep recurrent neural network approach to semantic segmentation,” *IEEE Transactions on Image Processing*, vol. 27, no. 5, pp. 2393–2407, 2018.

[42] K. Gregor and Y. LeCun, “Learning fast approximations of sparse coding,” in *Proceedings of the 27th International Conference on International Conference on Machine Learning*. Omnipress, 2010, pp. 399–406.

[43] M. Everingham, L. Van Gool, C. K. Williams, J. Winn, and A. Zisserman, “The pascal visual object classes (voc) challenge,” *International journal of computer vision*, vol. 88, no. 2, pp. 303–338, 2010.

[44] B. Hariharan, P. Arbeláez, L. Bourdev, S. Maji, and J. Malik, “Semantic contours from inverse detectors,” in *2011 International Conference on Computer Vision*. IEEE, 2011, pp. 991–998.

[45] P. Christ, “Lits liver tumor segmentation challenge (lits17).” [Online]. Available: <https://competitions.codalab.org/competitions/17094>

[46] B. H. Menze, A. Jakab, S. Bauer, J. Kalpathy-Cramer, K. Farahani, J. Kirby, Y. Burren, N. Porz, J. Slotboom, R. Wiest *et al.*, “The multimodal brain tumor image segmentation benchmark (brats),” *IEEE transactions on medical imaging*, vol. 34, no. 10, p. 1993, 2015.

[47] B. Kim and J. C. Ye, “Cycle-consistent adversarial network with polyphase u-nets for liver lesion segmentation,” 2018.

[48] F. Yu and V. Koltun, “Multi-scale context aggregation by dilated convolutions,” *arXiv preprint arXiv:1511.07122*, 2015.